

Numerical Analysis of Load-sharing Behavior of Combined Pile Raft Foundation System

Bhim Kumar Dahal^{1*}, Bikram Paudel¹, Archana Pandit², Aastha Pathak¹, Anil Mahat¹, Binayaraj Shrestha¹, Binit Banstola¹, Bipin Chhantyal¹, Diwash Dahal³

¹Department of Civil Engineering, Institute of Engineering, Pulchowk Campus, Tribhuvan University, Nepal

²Chulalongkorn University, Thailand

³Department of Civil Engineering, Southern Illinois University, Edwardsville, IL 62026, US

*Corresponding Author: bhimd@pcampus.edu.np

Abstract

This study investigates the application of combined pile raft foundations in the soft soil of Kathmandu Valley, taking into account varying pile spacing and length. Both embedded beams and volume piles were used in numerical analysis to assess the load-sharing behavior of the raft and pile under different conditions. The settlement results from the volume pile, and embedded beam element was comparable, with less than a 6.21% difference, indicating that both methods are equally suitable for evaluation. The embedded beam element was selected for further analysis. The analysis suggests that pile load sharing is primarily influenced by spacing, while an increase in pile stiffness due to increased pile length has a minor effect. The load-sharing factor follows a log-linear relationship when the spacing exceeds 3D. Regarding the normalized vertical settlement of the pile, the power rule governs the load-sharing factor. This power function related to normalized settlement is highly beneficial for designing the CPRF and choosing the appropriate pile spacing and length. Finally, the capacity utilization curve suggests that a spacing greater than three times the diameter results in higher pile capacity utilization. Conversely, a decrease in spacing significantly reduces the mobilized strength of the piles.

Keywords: Load sharing, Numerical analysis, Performance evaluation, Pile raft foundation, Soft soil

Introduction

The Kathmandu Valley, located at the heart of Nepal, is shaped by the meeting of two significant tectonic plates: the Indian Plate and the Eurasian Plate (Sharma et al., 2017). Its distinct geological features are shaped by various lacustrine sediments, comprising gravel, sand, silt, and clay, deposited over time (Bhattarai et al., 2017). The valley, an ancient settlement of Nepal, displays a blend of traditional and modern construction methods. Traditional Nepalese architecture commonly relies on stone and masonry foundations, featuring intricate carvings in historic structures, while contemporary approaches incorporate materials like reinforced concrete and steel. The combination of these constructions raises concerns regarding seismic resilience and preserving the region's architectural heritage (Hafner et al., 2023). In constructing infrastructure within the Kathmandu Valley, the choice of foundation is critical, influenced by geology, groundwater levels, and seismic risks (Carpenter & Grünwald, 2016). Additionally, geological formations have significantly shaped the area's architectural evolution. For instance, the Swayambhunath Stupa, a revered religious monument, exemplifies this adaptation, with its foundation tailored to local soil conditions, showcasing the skill of traditional builders in integrating structural stability with geological context (Chamlagain & Gautam, 2015). Conversely, insufficient foundations and structural elements have led to disasters like the collapse of the Dharahara Tower during the 2015 Gorkha earthquake, highlighting the importance of robust foundation systems (Suwal, 2018).

Raft foundations become necessary when the soil lacks strength or sufficient load-bearing capacity (Elwakil & Azzam, 2016). Raft foundations excel at distributing the load over a larger area, making them ideal for multi-story structures (Azhar et al., 2020). The presence of weak soil and seismicity of the Valley necessitate a more robust foundation solution, with alternatives like pile foundations, combined pile raft foundations (CPRF), or ground improvement beneficial for weak soil or large infrastructure such as tall buildings and bridges (El-Garhy et al., 2013; Acharya et al., 2023; Dahal et al., 2019).

CPRF uniquely combines the advantages of pile and raft foundations. Piles are crucial in transferring the structure's load to deeper, more stable soil layers. At the same time, the raft foundation component ensures uniform load distribution across a broader base area, catering specifically to larger structures like tall buildings and bridges (Hafner et al., 2023). Therefore, this topic is of paramount importance due to the complex geotechnical conditions and seismic vulnerability of Kathmandu Valley. As high-rise construction surges in urban areas, understanding how pile-raft foundation systems perform in this region is critical for ensuring structural stability and safety during earthquakes.

Objectives

The objective of this study is to evaluate the load-sharing behavior of combined pile raft foundations (CPRF) in the unique soil conditions of the Kathmandu Valley. By conducting numerical analyses with varying pile spacing and lengths using both embedded beam and volume pile models. The research aims to assess how these configurations influence settlement and load distribution.

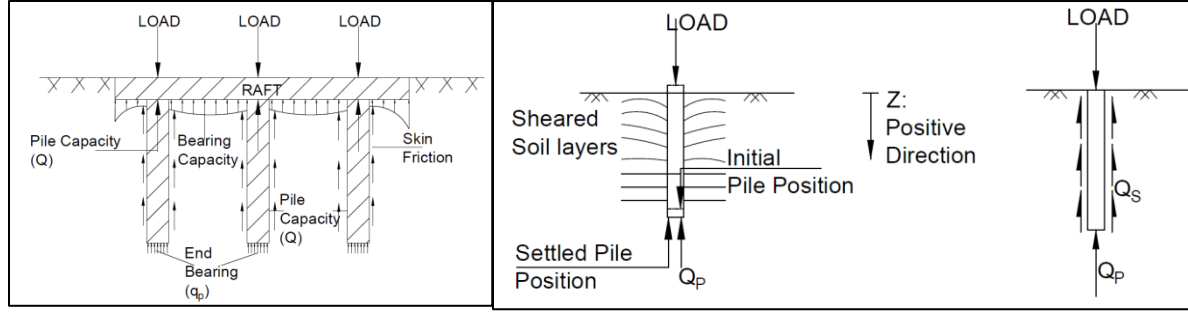
Literature review

Raft foundations involve a solid slab spanning the entire building's footprint, with bearing capacity dependent on the soil type. For cohesionless soil, Terzaghi's theory is often used to calculate ultimate bearing capacity, factoring in bearing capacity coefficients and unit weight (Terzaghi et al., 1996). For cohesive soil, Skempton's equations are commonly employed to determine net ultimate bearing capacity, considering cohesion, foundation depth, and raft dimensions. While there are several methods to calculate ultimate bearing capacity, these are among the most widely used. This approach allows for more efficient load distribution and can be especially beneficial in regions with challenging geotechnical conditions (Monaco et al., 2006).

The CPRF combines pile and raft systems to address soil challenges (Poulos et al., 2011). Piles are driven into the soil, transmitting loads to a stable stratum. A concrete raft atop the piles distributes the load widely. The CPRF's combines the unpiled raft and pile group capacities, incorporating interaction factors reflecting component-subsoil relationships (Poulos et al., 2011). Raft foundations offer uniform support to the entire building structure, ensuring that no individual section of the building experiences significantly differential settlement compared to other parts. This uniformity is critical for maintaining the structural integrity and safety of the building, especially in areas with soft or heterogeneous soils (Poulos et al., 2011).

Analysis approach of CPRF

One of the primary functions of a raft foundation is to distribute the structural load of a building evenly across a wide area of soil. In soft or compressible soils, traditional shallow foundations like isolated or strip footings may experience excessive settlement or differential settlement, leading to structural instability. Raft foundations help prevent these issues by spreading the load, minimizing the pressure on the underlying soft soil, and reducing the risk of settlement (Baban, 2016). A schematic diagram of the load shearing mechanism of CPRF and a single pile is presented in Figure 1, (a) and (b). Moreover, El-Garhy et.al. (2013) have observed that strategically placing even a few piles beneath the center of the raft can substantially bolster the foundation's load-bearing capacity (El-Garhy et al., 2013). Lee et al (2014) proposed load-sharing model elucidates that the sharing ratio diminishes as settlement ensues (Lee et al., 2014). Unsever et al. (2015) explored the influence of varying load levels and the interaction of foundation components (Unsever et al., 2015).



(a) Load sharing behavior of CPRF

(b) Load transfer behavior of single pile

Figure 1: Load transfer mechanism of CPRF and single pile

Raft pile interaction

The load-bearing capacity of the CPRF is assessed by integrating both the pile group's and un-piled raft's capacities. This comprehensive assessment involves considering various interaction factors, such as Pile-Raft and raft-pile interactions, to determine the foundation's overall strength and stability (Sinha, 2013). Additionally, the stiffness of the raft plays a pivotal role in its ability to distribute loads effectively. Stiffness calculations based on factors like Young's modulus, length, and thickness provide critical insights into the raft's load-bearing behavior, allowing for accurate predictions of its response to external forces (Hejazi et al., 2023). Load-bearing capacity of CPRF is given by Eq. (1).

$$Q_{\text{CPRF}} = \alpha_{\text{rp}} \alpha_{\text{pp}} \sum Q_{\text{single pile}} + (\alpha_{\text{pr}} * Q_{\text{unpiled raft}}) \quad (1)$$

Where, Q_{CPRF} =load-bearing capacity of the CPRF, $Q_{\text{single pile}}$ =load-bearing capacity of a single pile, $Q_{\text{unpiled raft}}$ =load-bearing capacity of the un-piled raft, α_{pr} =pile-raft interaction factor, α_{rp} =raft-pile interaction factor, and α_{pp} =pile-pile interaction factor.

The pile-pile interaction is the result of the pile group effect, defined as the changes in the load-settlement response of a pile group and single piles due to the superimposition of stress and displacement field of a single pile in a group (Kumar & Choudhury, 2018). Load carrying capacity of a single pile can be used to calculate load bearing capacity of the pile group using this interaction factor as $Q_{\text{group pile}} = \alpha_{\text{pp}} \sum n(Q_{\text{singlepile}})$

Similarly, load settlement of the pile group changes when the raft is placed above the pile group. The load-carrying capacity of the pile group in CPRF ($Q_{\text{P-CPRF}}$) is influenced by the pile-raft interaction factor as shown in Eq. (2).

$$Q_{\text{P-CPRF}} = \alpha_{\text{pr}} * Q_{\text{group pile}} \quad (2)$$

The estimation of this interaction considering both negative and positive aspects is very complex. The predicted values of α_{pr} were limited to unity for conservatism in the design and expressed in Eq. (3).

$$\alpha_{\text{pr}} = \left(\frac{Q_{\text{P-CPRF}}}{Q_{\text{group pile}}} \right) = 1 - \exp \left(-10.55 \left(\frac{S_z}{B_r} \right)^{0.26} \right) \quad (3)$$

Here, S_z and B_r are settlement and width of raft respectively. The load carrying capacity of the raft changes when a pile is introduced below the raft. The load-carrying capacity of a raft of CPRF ($Q_{\text{R-CPRF}}$) can be computed in terms of load carrying capacity of an unpiled raft using this factor as shown in Eq. (4).

$$Q_{\text{R-CPRF}} = \alpha_{\text{rp}} * (Q_{\text{unpiled raft}}) \quad (4)$$

α_{rp} is expressed as the ratio of load carrying capacity of CPRF to the summation of the load-bearing capacity of the un-piled raft and the pile group (Kumar & Choudhury, 2018).

$$\alpha_{rp} = \left(\frac{Q_{R-CPRF}}{Q_{unpiled\ raft}} \right) = \eta + (\eta - \alpha_{rp}) * \left(\frac{Q_{PG}}{Q_{UR}} \right) \quad (5)$$

The value of η is calculated for all the configurations which indicate an increase in η with an increase in the normalized settlement as $\eta = 3.5 \left(\frac{S_z}{B_r} \right) - 0.06 \left(\frac{S}{D_p} \right) - \frac{0.5}{D_p} + 1.27$ (6)

Numerical analysis

Several studies have shed light on the behavior of pile raft foundations (CPRF) under seismic conditions. Elwakil & Azzam (2016) found that shorter piles exacerbate raft loading during significant ground motion (Elwakil & Azzam, 2016). Kumar, Choudhury, & Katzenbach (2016) conducted centrifuge tests and numerical analyses, determining that maximum bending moment and displacement occur at the pile head (Kumar et al., 2016). Sinha & Hanna (2017) explored the impact of pile spacing on raft settlement (Sinha & Hanna, 2017), while Chandiwala & Vasanwala (2018) used 3D models to investigate settlement and load-sharing in layered soil structures (Chandiwala & Vasanwala, 2018). Deb & Pal (2019) developed predictive models to understand load-sharing and interaction effects (Deb & Pal, 2019), while Azhar, Patidar, & Jaurker (2021) examined how varying parameters affect stress and settlement in layered soil (Azhar et al., 2020). Hejazi (2023) conducted a detailed study using finite element analysis to explore superstructure foundation behavior (Hejazi et al., 2023), and Shamsi Sosahab and his team performed a numerical analysis on piled raft foundations using FLAC 3D (Shamsi Sosahab et al., 2019).

However, there's a gap in research regarding CPRF in Kathmandu soil. Only one study, by Niraula and Acharya (2021), has been conducted on CPRF in Kathmandu Valley, considering the constant spacing of pile (Niraula & Acharya, 2021). While a study conducted on analysis of the pile foundation reported that the spacing of pile significantly affects the performance of pile foundation (Gupta & Dahal, 2023). Therefore, studying CPRF response and load-sharing behavior in Kathmandu Valley soil is important, it is also crucial to explore other comprehensive foundation types to gain a holistic understanding of the soil characteristics and foundation performance in this region.

Methodology

The evaluation approach for a Combined Piled-Raft Foundation (CPRF) system encompasses three key elements: geometric factors, material characteristics, and finite element analysis. These components offer a comprehensive understanding of the system's performance, revealing important details about its structural integrity and load-bearing capacity.

Geometry

The geometric configuration of the foundation plays a crucial role in its overall performance. To assess this, various factors, both fixed and variable, were considered, as presented in Table 1 and Figure 2. These geometric parameters collectively form the basis for understanding the intricate interplay between structural components and their surrounding environment, contributing to a holistic system analysis (Katzenbach et al., 2016).

Table 1: Geometry considered for numerical modeling

Element	Description	Value
Raft	Raft from Ground Surface (m)	2.5
	Thickness, T (m)	0.6

	Length, L (m)	36
	Breadth, B (m)	36
Pile	Diameter, D (m)	1
	Length, L (m)	6D,9D,12D,15D
	Spacing, S (m)	2D,3D,4D,6D,10D
Model size	X_{min} (m)	-50
	Y_{min} (m)	-50
	X_{max} (m)	50
	Y_{max} (m)	50
	Z_{min} (m)	-30

Water Table Influence: The proximity of the water table, situated 3 m beneath the ground surface, significantly impacts soil mechanical properties and potential interactions with structural elements.

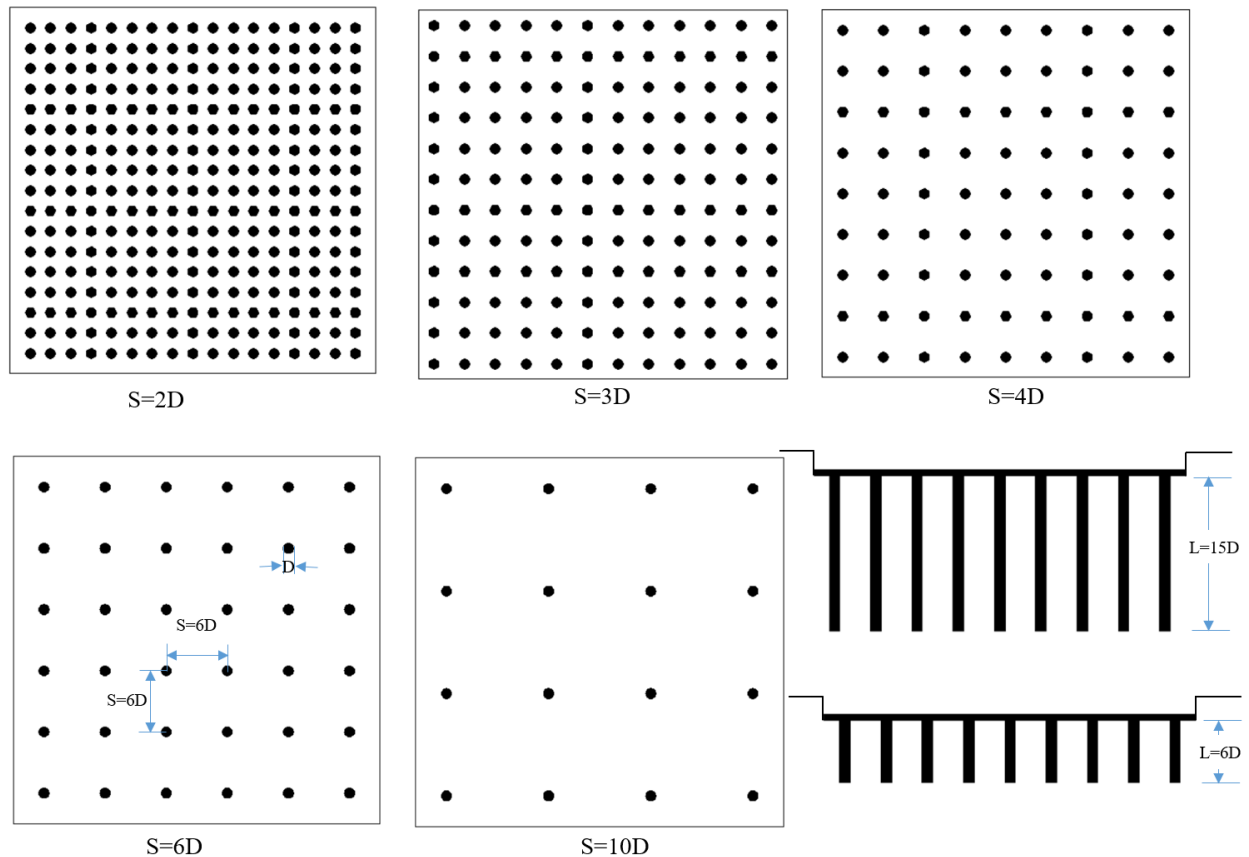


Figure 2: Geometric arrangement of CPRF; arrangement with different spacing and different lengths of piles

Materials

An in-depth understanding of material properties is essential for evaluating the foundation's performance. The soil sample collected from a borehole in Chakupat, Lalitpur. Laboratory tests were conducted to

determine essential soil parameters, including water content, specific gravity, density, and strength characteristics. The soil is classified as loam (Textural Classification), A-4(0) (AASHTO classification), and low plasticity inorganic silt (Unified Classification). The shear strength parameters derived from the Direct Shear Test are a cohesion (C) of 13.86 kPa and a friction angle of 25.58°.

Table 2: Soil properties

Category	Property	Value
Basic Parameters	Water Content (%)	30.34
	Specific Gravity	2.469
	Bulk Density (kg/m ³)	1745
	Dry Density (kg/m ³)	1339
	Liquid Limit (%)	36.33
	Plastic Limit (%)	29.21
	Plasticity Index (%)	7.12
Particle Size Distribution	Gravel (%)	0.40
	Sand (%)	49.70
	Silt (%)	40.60
	Clay (%)	9.30
Strength	Cohesion, c (kPa)	13.86
	Friction Angle, Φ (°)	25.58
Stiffness	E (kPa)	3315
	ν	0.267

Table 3: Raft and pile parameters

Property	Value
Material Model	Linearly Elastic
Unit Weight, γ (kN/m ³)	25.00
Elastic Modulus, E (kPa)	2.78E+07

Finite Element Analysis

The Finite Element Analysis (FEA) using PLAXIS 3D involved several critical stages. It began with formulating the geometry and meshing the model, which included defining the soil layers, structural components such as raft and pile, and relevant boundary conditions, as detailed in Table 1. In the study by Nasasira and Srivastava on the Effect of Mesh Size on Soil-Structure Interaction in Finite Element Analysis, the influence of mesh size on model precision and computational efficiency is thoroughly investigated. While mesh size is a crucial parameter affecting model accuracy, it is recognized that other factors such as the choice of FEM solver and mesh type also play significant roles in numerical simulations of soil-structure interactions (Nasasira Derrick, 2020). The study underscores the importance

of conducting sensitivity analyses to optimize these parameters for accurate predictions in geotechnical applications. Similarly, a crucial aspect of FEA is the assignment of appropriate material properties to each element within the model. These incorporate parameters like soil stiffness, strength, and other pertinent attributes. The model properties are presented in **Table 2** and **Table 3**.

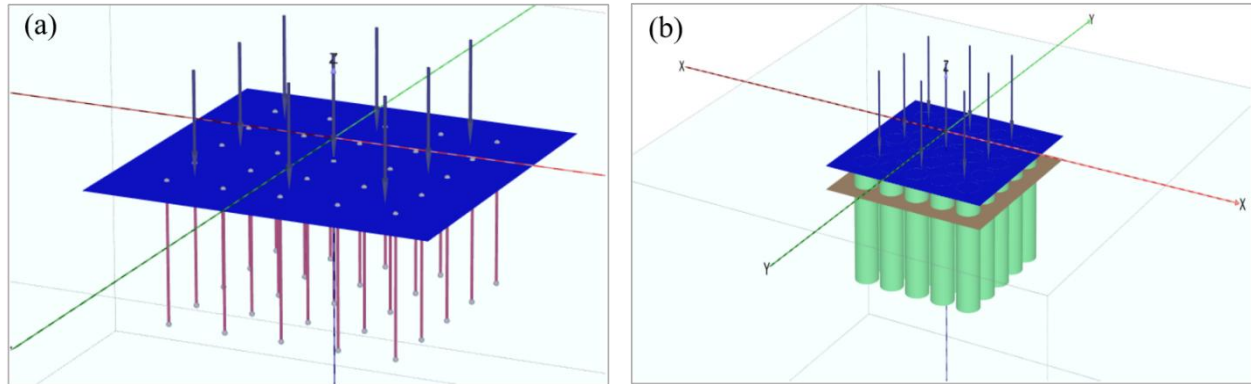


Figure 3: Finite element modeling of pile in CPRF: a) Embedded beam, and b) Volume pile

The soil layer is modeled with the Mohr-Coulomb constitutive model while the raft of the foundation is modeled with the linear elastic material model. Similarly, the pile is modeled with the embedded beam model and the volume pile. Defining the material model, loading, boundary condition, and construction sequence are the most important stages of FEA. Moreover, the analysis method, time steps, and convergence criteria were tailored to suit the simulation. This methodology serves as a robust framework for evaluating the performance and load-bearing capacity of the CPRF system and comparing the results with different modeling processes of the pile in the soil from Kathmandu Valley.

Results and Discussion

The study utilized the embedded beam model to simulate piles with various configurations of pile spacing (2D, 3D, 4D, 6D, and 10D) and lengths (6D, 9D, 12D, and 15D). A volume pile model was also employed for comparative analysis, explicitly focusing on 6D spacing and varying lengths (6D, 9D, 12D, and 15D). The settlement data obtained from both models, particularly for a spacing of 6D and different lengths, is illustrated in Figure 4. Remarkably, settlements in both models exhibit similar trends, with a maximum difference of only 6.21% observed for a pile length of 9D, gradually decreasing to 4.49% for a length of 15D. Consequently, the findings derived from the embedded beam model are deemed suitable for further analysis of CPRF and are elaborated upon in subsequent discussions.

Figure 5 illustrates the relationship between settlements with the spacing and the length of the piles. The graph demonstrates that by increasing the pile spacing in CPRF, the settlement also increases. For a pile length equal to 9D, increasing the spacing from 2D to 3D led to an increase in settlement by 7.86mm, i.e., a 12.98% increment in the settlement. Furthermore, when the spacing was increased from 6D to 10D, a significant increase in settlement was observed, i.e., 47.68mm, which equals to 50.43% increment. However, the change in the settlement in the spacing is less than 4D. This infers that closely spaced piles increase the number of piles in the foundation, resulting in the overlap of the pressure bulb and causing relatively higher settlement. Upon increase in the spacing, the overlap of the pressure bulb decreases, causing the increased efficiency of the pile, resulting in less increment in the settlement. After spacing more than 4D, the increases in the spacing cause decreases in the pile number, resulting in lower load-carrying capacity and higher settlement.

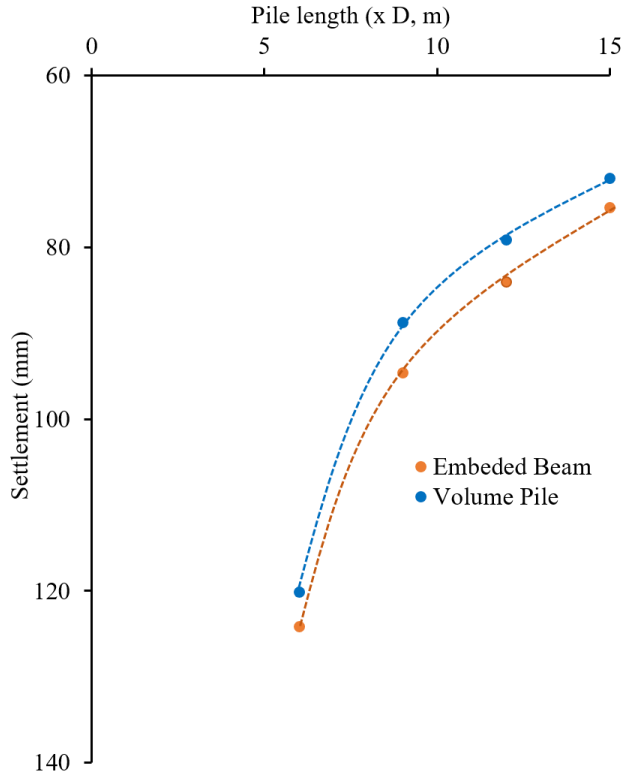


Figure 4: Comparison of settlement with different pile models

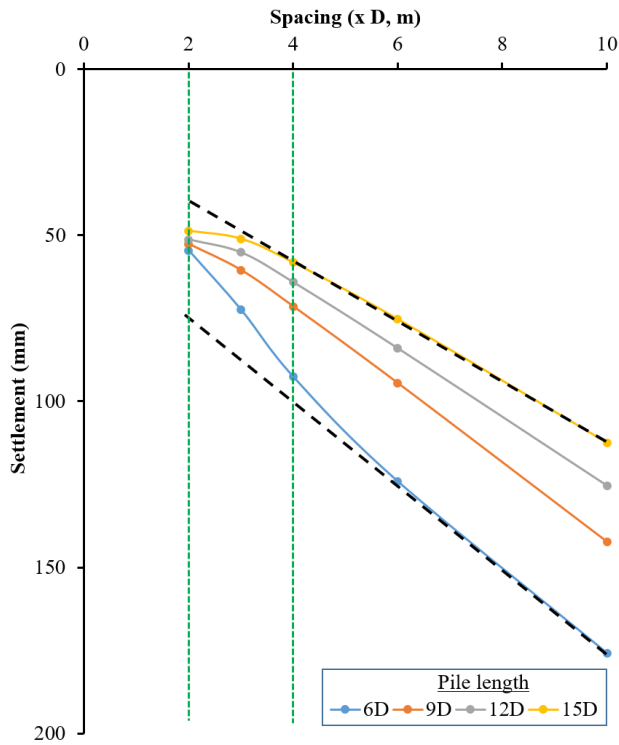


Figure 5: Variation of settlement with length and spacing of piles

Similarly, to analyze the settlement of CPRF with pile length, various piles with lengths of 6D, 9D, 12D, and 15D were considered for each spacing. It demonstrates that the settlement of the CPRF decreases as the length of the piles increases. However, it should be noted that the effectiveness of settlement reduction differs for various increases in pile length at different spacing. For instance, in the case of a spacing of 6D, when the pile length is increased from 6D to 9D, the settlement is significantly reduced by 29.53mm, which corresponds to approximately 23.8% reduction compared to the original value. On the other hand, for the same spacing, when the pile length is increased from 12D to 15D, the settlement reduction is decreased by only 8.73mm, which accounts for only a 10.39% reduction of the settlement.

Load sharing behavior

To analyze the load-sharing behavior of CPRF with different pile spacing and lengths, a constant surface load of 100 kN/m² was applied to the raft surface. The results indicate that as the spacing between piles increases, resulting in fewer piles, the percentage of load carried by the piles decreases (see Figure 6). For instance, when the pile spacing is 2D, and the pile length is 6D, the percentage of load taken by the piles amounts to 71.28%. However, increasing the spacing to 10D reduces this percentage significantly to 46.38%. The reduction in load sharing when the pile length exceeds 9D follows a declining trend, as illustrated in Figure 6, suggesting that the most optimal pile spacing is around 3D, as found in most of the literature. Similarly, Figure 6 shows that as the depth of the piles in the CPRF increases, the percentage of load taken by the piles also increases. Piles with lengths of 6D, 9D, 12D, and 15D were tested with different spacing. For instance, with a pile spacing of 3D and a pile length of 6D, the percentage of load taken by the piles is 64.33%. However, as the pile length increases to 9D, 12D, and 15D, the percentage of load taken by the piles also increases to 68.64%, 71.06%, and 73.07%, respectively.

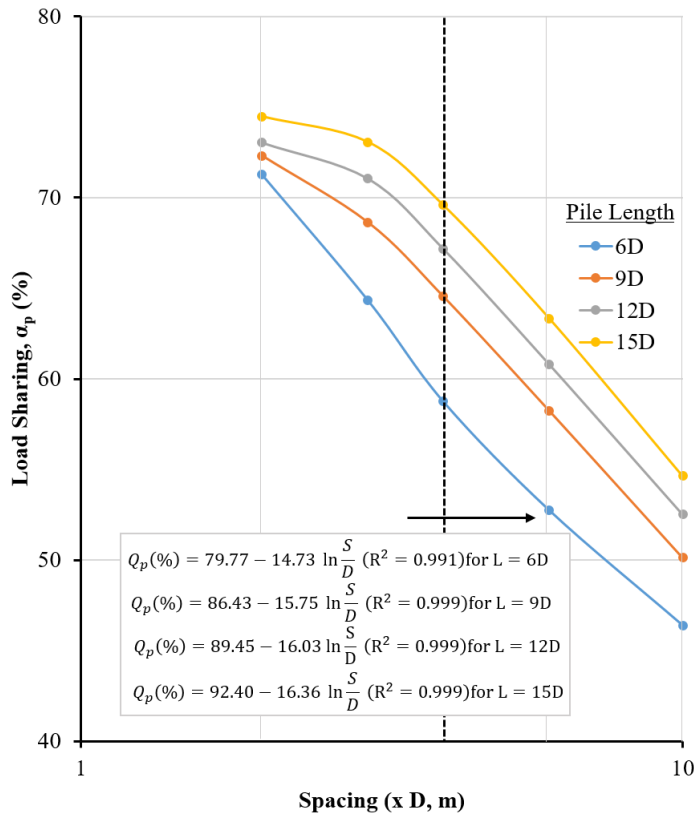


Figure 6: Load sharing with variation of length and spacing of piles

Figure 7 illustrates that the load sheared by piles across various configurations, including different spacing (2D, 3D, 4D, 6D, 10D) and lengths (6D, 9D, 12D, 15D), with normalized settlement ($\frac{s_z}{B_r}$). This analysis reveals that the load distribution of CPRF is influenced by the permissible settlement of the foundation, as defined by a power function of the normalized settlement. For instance, if the permissible total settlement is 1 in 400, the load sheared by piles totals to 59.13%. However, as settlement increases, the load carried by the raft increases accordingly. Therefore, it's crucial for designers to consider this behavior and arrange piles accordingly to ensure optimal performance.

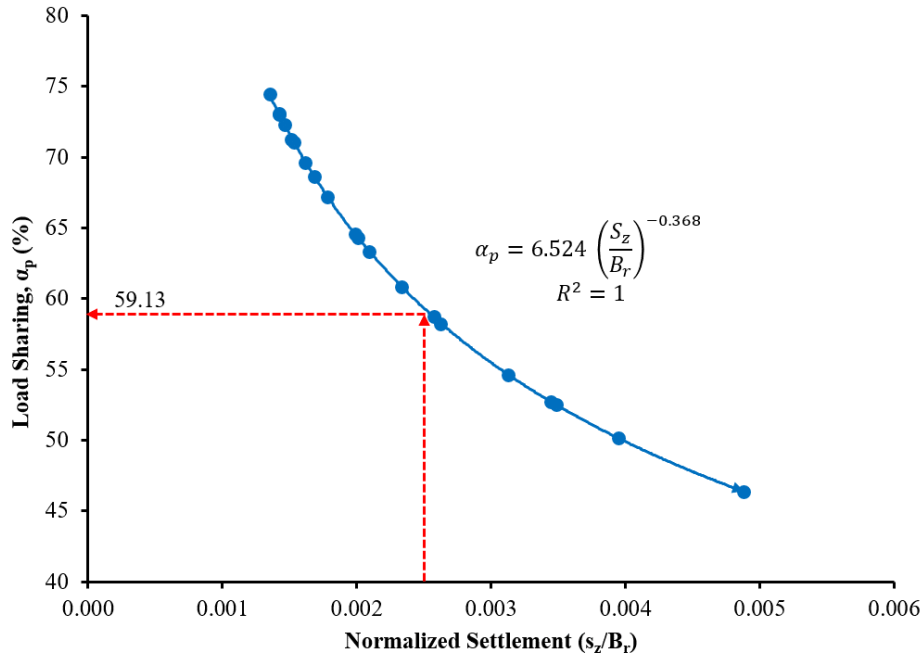


Figure 7: Load sharing with variation of length and spacing of piles

Capacity utilization

Figure 8 illustrates the significance of pile spacing in the overall capacity utilization of piles, whereas the pile length appears to play a negligible role. The graph depicts a gradual increase in capacity utilization up to a spacing of 4D, beyond which the load on individual piles follows a log-linear pattern, as evidenced in Figure 8. The marginal increase in load due to the increase in the length of the pile primarily stems from enhanced pile stiffness. Furthermore, Table 4 illustrates the load taken by a pile across various spacing intervals and lengths. The findings reveal that doubling the spacing from 2D to 4D results in an approximately threefold increase in pile load. Moreover, the capacity utilization experiences a substantial increase of approximately twelvefold when the spacing is increased to 10D.

Table 4: Load taken by a pile for different spacing and lengths (kN)

Spacing	2D	3D	4D	6D	10D
Number of piles	289	144	81	36	16
6D	319.65	578.97	940	1898.64	3756.78
9D	324.31	617.76	1032.96	2097	4060.53
12D	327.59	639.54	1075.04	2189.16	4253.31
15D	334.00	657.63	1113.44	2280.24	4425.03

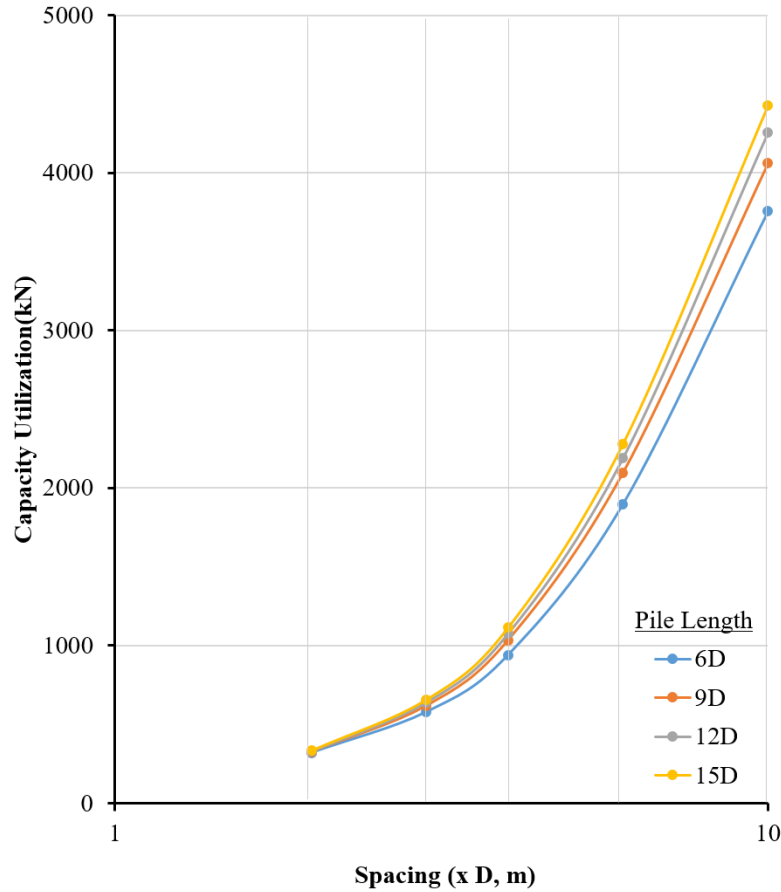


Figure 8: Pile capacity utilization with variation of length and spacing of piles

Conclusions

The research on the combined pile raft foundation system in the soft soil deposit of Kathmandu Valley, using various pile configurations and pile element modeling in Plaxis 3D, has led to the following conclusions:

- The study indicates that an increase in spacing and a decrease in the number of piles results in an increased settlement of the combined pile raft foundation. However, extending the length of the piles for the same spacing leads to a decrease in settlement. A slight variation in results was observed when comparing the modeling of piles as volume elements and embedded beam elements.
- The research also found that a decrease in spacing and an increase in the number of piles results in an increased percentage of load carried by the piles in the combined pile raft foundation. The relationship between load shearing and spacing is log-linear for spacing greater than 3D ($\alpha_p (\%) = a - b \ln \frac{S}{D}$), and the results are more pronounced when the pile length is greater than 9D.
- Furthermore, the load shearing behavior of the CPRF has a strong correlation with the settlement, represented by the equation $\alpha_p = 6.524 \left(\frac{S_z}{B_r} \right)^{-0.368}$. This relationship is crucial in designing the spacing and the length of the pile in CPRF.

The findings of this study, along with the established correlations, provide a reliable design approach for constructing large infrastructures in areas with soil of low bearing capacity, using an appropriate design and optimized arrangement of piles. However, as the soil used in this study is from a single location, further research is needed for generalization.

References

- Acharya, S., Niraula, U., & Dahal, B. K. (2023). Improving Soft Clay Behavior with Alkali-Activated Waste Eggshell for Sustainable Ground Engineering. *International Journal of Geosynthetics and Ground Engineering*, 9(5), 1–13. <https://doi.org/10.1007/s40891-023-00480-9>
- Azhar, S., Patidar, A., & Jaurker, S. (2020). Parametric Study of Piled Raft Foundation for High Rise Buildings. *International Journal of Engineering Research & Technology (IJERT)*, 9(12), 548–555. www.ijert.org
- Baban, T. M. (2016). *Shallow Foundations*. Wiley. <https://doi.org/10.1002/9781119056140>
- Bhattarai, R., Alifu, H., Maitiniyazi, A., & Kondoh, A. (2017). Detection of Land Subsidence in Kathmandu Valley, Nepal, Using DInSAR Technique. *Land*, 6(2), 39. <https://doi.org/10.3390/land6020039>
- Carpenter, S., & Grünewald, F. (2016). Disaster preparedness in a complex urban system: the case of Kathmandu Valley, Nepal. *Disasters*, 40(3), 411–431. <https://doi.org/10.1111/disa.12164>
- Chamlagain, D., & Gautam, D. (2015). *Seismic Hazard in the Himalayan Intermontane Basins: An Example from Kathmandu Valley, Nepal* (Issue October). https://doi.org/10.1007/978-4-431-55242-0_5
- Chandiwala, A. K., & Vasanwala, S. A. (2018). A parametric study on behaviour of piled raft foundation-structure interaction effects on seismic performance of multi-story regular rc mrf building. *International Journal of Civil Engineering and Technology*, 9(7), 558–567.
- Dahal, B. K., Zheng, J. J., Zhang, R. J., & Song, D. B. (2019). Enhancing the mechanical properties of marine clay using cement solidification. *Marine Georesources and Geotechnology*, 37(6), 755–764. <https://doi.org/10.1080/1064119X.2018.1484532>
- Deb, P., & Pal, S. K. (2019). Analysis of Load Sharing Response and Prediction of Interaction Behaviour in Piled Raft Foundation. *Arabian Journal for Science and Engineering*, 44(10), 8527–8543. <https://doi.org/10.1007/s13369-019-03936-1>
- El-Garhy, B., Galil, A. A., Youssef, A. F., & Raia, M. A. (2013). Behavior of raft on settlement reducing piles: Experimental model study. *Journal of Rock Mechanics and Geotechnical Engineering*, 5(5), 389–399. <https://doi.org/10.1016/j.jrmge.2013.07.005>
- Elwakil, A. Z., & Azzam, W. R. (2016). Experimental and numerical study of piled raft system. *Alexandria Engineering Journal*, 55(1), 547–560. <https://doi.org/10.1016/j.aej.2015.10.001>
- Gupta, S. K., & Dahal, B. K. (2023). Finite Element Analysis on Load-Settlement Behavior of Axially Loaded Pile on Sand. *Journal of Engineering Technology and Planning*, 4(1), 72–81. <https://doi.org/10.3126/joetp.v4i1.58443>
- Hafner, I., Kišiček, T., & Gams, M. (2023). Review of Methods for Seismic Strengthening of Masonry Piers and Walls. *Buildings*, 13(6). <https://doi.org/10.3390/buildings13061524>
- Hejazi, S. A. M., Feyzpour, A., Khaje khabaz, M., Eslami, A., Fouladgar, M., Eftekhari, S. A., & Toghraie, D. (2023). Numerical investigation of rigidity and flexibility parameters effect on superstructure foundation behavior using three-dimensional finite element method. *Case Studies in Construction Materials*, 18(October 2022), e01867. <https://doi.org/10.1016/j.cscm.2023.e01867>
- Katzenbach, R., Leppla, S., & Choudhury, D. (2016). Foundation systems for high-rise structures. *Foundation Systems for High-Rise Structures, October*, 1–298. <https://doi.org/10.1201/9781315368870>
- Kumar, A., & Choudhury, D. (2018). Development of new prediction model for capacity of combined pile-raft foundations. *Computers and Geotechnics*, 97(October 2017), 62–68. <https://doi.org/10.1016/j.compgeo.2017.12.008>
- Kumar, A., Choudhury, D., & Katzenbach, R. (2016). Effect of Earthquake on Combined Pile–Raft Foundation. *International Journal of Geomechanics*, 16(5), 1–16. [https://doi.org/10.1061/\(asce\)gm.1943-5622.0000637](https://doi.org/10.1061/(asce)gm.1943-5622.0000637)
- Lee, J., Park, D., & Choi, K. (2014). Analysis of load sharing behavior for piled rafts using normalized load response model. *Computers and Geotechnics*, 57, 65–74. <https://doi.org/10.1016/j.compgeo.2014.01.003>
- Monaco, P., Totani, G., & Calabrese, M. (2006). DMT-Predicted vs observed settlements: a review of the available experience. *Second International Flat Dilatometer Conference, April 2006*, 244–252.
- Nasasira Derrick, A. K. S. (2020). Effect of Mesh Size on Soil-Structure Interaction in Finite Element Analysis. *International Journal of Engineering Research And*, V9(06), 802–807. <https://doi.org/10.17577/ijertv9is060655>
- Niraula, S., & Acharya, I. P. (2021). Study on Parametric Analysis of Piled Raft Foundation System Using Finite Element Approach. *Journal of Advanced College of Engineering and Management*, 6, 143–157. <https://doi.org/10.3126/jacem.v6i0.38348>

- Poulos, H. G., Small, J. C., & Chow, H. (2011). Piled raft foundations for tall buildings. *Geotechnical Engineering*, 42(2), 78–84.
- Shamsi Sosahab, J., Jamshidi Chenari, M., Jamshidi Chenari, R., & Karimpour Fard, M. (2019). Physical and Numerical Modeling of Piled Raft Foundation in Chamkhaleh Sand. *International Journal of Civil Engineering*, 17(6), 765–779. <https://doi.org/10.1007/s40999-018-0365-1>
- Sharma, K., Subedi, M., Parajuli, R. R., & Pokharel, B. (2017). Effects of surface geology and topography on the damage severity during the 2015 Nepal Gorkha earthquake. *Lowland Technology International*, 18(4), 269–282.
- Sinha, A. (2013). 3-D Modeling of Piled Raft Foundation. *March*, 235.
- Sinha, A., & Hanna, A. M. (2017). 3D Numerical Model for Piled Raft Foundation. *International Journal of Geomechanics*, 17(2), 1–9. [https://doi.org/10.1061/\(asce\)gm.1943-5622.0000674](https://doi.org/10.1061/(asce)gm.1943-5622.0000674)
- Suwal, R. (2018). Failure Study of Reinforced Concrete Buildings of Kathmandu Valley In Gorkha Earthquake 2015. *International Journal of Modern Research in Engineering & Management (IJMREM) ||Volume||, May 2018*, 2581–4540. www.ijmrem.com
- Terzaghi, K., Peck, R. B., & Mesri, G. (1996). Plastic equilibrium in soils. In *Soil mechanics in engineering practice* (pp. 258–262).
- Unsever, Y. S., Matsumoto, T., & Özkan, M. Y. (2015). Numerical analyses of load tests on model foundations in dry sand. *Computers and Geotechnics*, 63(June 2022), 255–266. <https://doi.org/10.1016/j.compgeo.2014.10.005>